Available online at www.sciencedirect.com

ScienceDirect

Procedia Materials Science 12 (2016) 106 – 111

Procedia Materials Science

www.elsevier.com/locate/procedia

6th New Methods of Damage and Failure Analysis of Structural Parts [MDFA]

Response of alumina foam to tensile mechanical loading including stress concentrator effect

Ivo Dlouhy[a]*, Zdenek Chlup[a], Hynek Hadraba[a], Lukas Rehorek[b]

[a]*Institute of Physics of Materials ASCR, CEITEC IPM, Zizkova 22, 61662 Brno, Czech Republic*
[b]*Military Research Institute, Division of Materiasl Engineering, Veslarska 230, 63700 Brno, Czech Republic*

Abstract

Tensile test methodology for ceramic foams has been elaborated and test specimens of different dimensions and those containing central sharp notch (simulating a crack) were tested. Tested material was commercially available alumina based ceramic foam commonly used as filters of light metals melts. The foam cell size used within this study was 60 PPI. The main aim of the investigation has been to prove experimentally whether there is any stress concentration effect in the open cell structures. The fracture load (tensile strength) values were analysed and, in particular, the samples containing central sharp notch and comparable unbroken cross-section were compared with the unflawed samples. Specimens with central through thickness sharp notch have shown demonstrably the strength values comparably lower than the strength level of samples having the same cross-sectional area without stress concentrator. The explanation has been seen in stress concentration effect beneath the internal sharp notch root.

Selection and peer-review under responsibility of the VŠB - Technical University of Ostrava,Faculty of Metallurgy and Materials Engineering

Keywords: Tensile Test, Ceramics Foam, Open Porosity, Strength, Stress Concentrators.

1. Introduction

Ceramic foams with open cell porosity structure are of the growing technological interest because of their potential use in a number of industrial branches. There are applications already proven like high temperature filters for melted alloys, by Taslicukur et al. (2007) or Patcas et al. (2007), insulation materials, e.g. Gibbson and Ashby

* Corresponding author. Tel.: +420 532 290 342; fax: +420 541 218 657.
E-mail address: idlouhy@ipm.cz

Selection and peer-review under responsibility of the VŠB - Technical University of Ostrava,Faculty of Metallurgy and Materials Engineering
doi:10.1016/j.mspro.2016.03.019

(1999), catalytic substrates by Garrido et al. (2008), Dawson et al. (2006), in tissue engineering also as bone replacement materials, Chen et al (2006), Bertolla et al. (2014a) and (2014b) etc. In almost all cases, high permeability, high surface area and good insulation characteristics but also a corresponding response to different types of mechanical loading is required for the given applications. In order to understand fully to mechanical response of ceramics foams it is necessary to cover all typical loading modes.

It is common to estimate behaviour of ceramic foams by compressive tests. A crushing strength is usually determined from the compression test curve. When a load is applied to the foam structure, it will initially deform elastically and then, depending on the sample size, the foam structure begins to buckle and collapse continuously at a relatively constant stress. Depending upon the initial foam relative density, this collapse will proceed under constant load up to a relatively high strain level. At a certain point the compressed foam enters to the "densification" phase and the stress - strain trace begins to rise. The point typical for transition from the elastic to plastic deformation phase defines the crush strength of the ceramic foam, Gibbson and Ashby (1999).

Very limited number of investigations has attempted also a bending test, e.g. Brezny and Green (1990). The most complication is associated with measures to avoid the crushing between the rollers and the examined foam. Suitable thin, usually rubber, sheet must be applied onto the interface between the roller and specimen surface. It must be rigid and tough but not too much to assure load transfer, Brezny and Green (1989).

Tensile loading always brings difficulties and data of tensile tests of the ceramic foams are completely missing in the literature. It is necessary to solve efficient load transfer from load fixture to specimen struts and ensure alignment of the specimen with loading axis of the test system. Brittleness of this type of material brings complications in fixating of the material in some claws. It is impossible to use any fixing methods exploiting compression, friction, threaded joint and their combinations. Only one possibility is to employ adhesion evoked by adhesive or resin, Rehorek et al. (2009). Another difficulty connected with the tensile testing of the brittle foam-like materials supposes measurement of deformations (tensile elongation, local displacements etc.). Direct placement of any contact strain gauge on the specimen is inapplicable due to risk of premature specimen surface damage. For interpretation of the mechanical behaviour and modelling the ceramic foam response in the given applications real material data are needed however, Marcian et al (2012). Thus noncontact methods are necessary.

The aim of the paper is seen in presentation of knowledge obtained with the tensile tests of ceramic foams carried out with different specimen size with and without internal through thickness crack. The question is whether there is any stress concentration effect at the crack tip of such artificial internal crack.

2. Experimental details

2.1. Material and specimen preparation

Alumina based foam (85 vol. % Al_2O_3, 14 vol. % SiO_2, 1 vol. % MgO) was applied for the tests. It has been a commercially produced material (Vukopor®A, produced by company Lanik, Czech Republic) typically used e.g. for melt aluminium alloys filtration. The material was produced by replication technique consisting of slurry coating of polyurethane foam. Typical for this kind of ceramic foam fabrication is highly porous structure with open type of porosity with triangular hole within the strut. Cell size used for this investigation was nominally 60 pores per linear inch (PPI), it corresponds to typical cell size of 0.8 (±0.3 mm), respectively. Fig. 1 shows distribution characteristics of the structure including SEM picture of the foam taken from the fracture surface. The distribution characteristics have been generated from quantitative analyses of computer 3D tomography pictures.

The material was provided in form of test specimens with agreed geometry having form of rectangular bars. The dimensions of specimens were 10x10x30 mm^3 (labelled as A), 15x15x40 mm^3 (B), and 30x30x90 mm^3 (C), 15x30x90 mm^3 (T). The last was also fabricated with the artificial through thickness sharp notch simulating a crack of the length 10 mm, i.e. remaining unbroken part having the area of 15x20 mm^2 (T-CR).

2.2. Test methodology

For loading of the above mentioned specimens the electromechanical machine ZWICK Z050 with 1 kN load cell controlled by TestXpert software was used. A special fixture and testing rig was developed, by Rehorek et al.

(2009); the specimen was embedded into two tusked aluminium pots by adhesive which ensured homogeneous transfer of load forces from the machine fixtures to the specimen struts. The adhesive medium used for fixation of specimen in the pot was Duracryl Plus (Spofa Dental, Czech Republic). Advantage of this solution is seen in easily controllable viscosity of fixative liquid and thereby controllable wettability of the specimens. The shrinkage of the adhesive during solidification and possible formation of tensile stresses imposed on the separate struts must be also taken into account as it has been analysed elsewhere. Difficulties connected with alignment of specimen and loading axis were solved by designing special aluminium pots holders. The upper holder was supplied with cardan shaft and claw which was mounted by pivot and lower claw was connected by a bulb to the shaft.

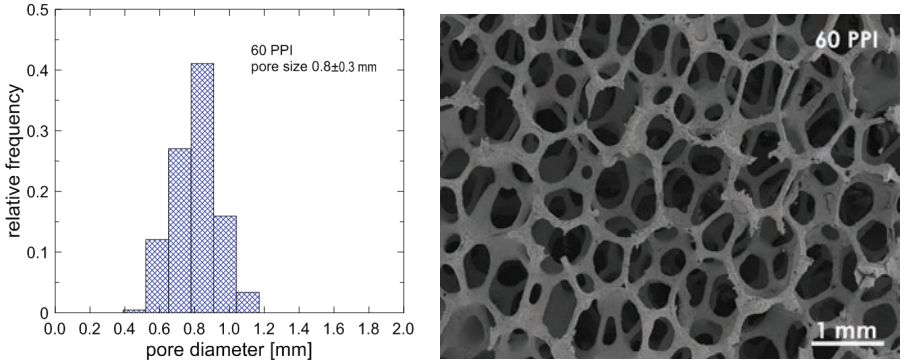

Fig. 1: Cell size distribution of ceramic foam investigated and SEM micrograph of the typical foam structure.

Cross-head speed of 0.1 mm/min was applied for the set of experiments reported here. The specimen elongation was measured by means of the noncontact documentation of the specimen surface by monochromatic laser beam and post mortem calculations of the local and global displacements based on digital image correlation method. In addition, in order to enable right interpretation of the geometrical changes of the sample during the tensile elongation in relation to the foam structure sequences of pictures have been collected from the specimen surface by digital high resolution camera in the fixed time intervals. During the test the timing of the load and specimen pictures was registered so the given picture can be exactly attributed to the loading stage of the specimen.

3. Results

3.1. Apparent tensile strength

For tensile test specimens without any artificial sharp defect it is possible to observe a linear increase of load up to fracture of the first strut (and/or several struts) suitably oriented to the acting load (usually the strut loaded in bending, Majer, 2012) reflected by pop-in on the trace. This strut fracture didn't lead to overall specimen fracture, however, and further increase of the load was possible to observe. The maximum load leads to the critical damage in the cell structure usually associated with the fracture of several cells and sudden drop of the load. This step is caused by fracture of several struts and obviously the whole specimen is broken at this stage.

Tensile strength values were determined as maximum force from the loading diagram related to cross-sectional area of the specimen at fracture. The cross-sectional area needed for this procedure was measured by digital picture capturing of the fracture surface of the samples by macro-objective with digital camera and by carrying out image analysis associated with corresponding dimensions measurement on both halves of the broken sample. The cross-sectional area contains more than 80% of unfilled space and estimation of the fracture strength is thus complicated; it doesn't correspond to real strength of the strut material but to some value corresponding to the response of the whole structure. Therefore further the fracture strength is marked as apparent tensile strength.

Average values of apparent strength determined for all types of the tested specimens are shown in Table 1. As expected, both the average values and the scatter of apparent tensile strength values are affected by specimen size.

Specimens with cross section of 15x15 mm^2 (B) and 30x30 mm^2 (C) showed noticeable lower data scatter thanks to larger sampling volume averaging the structural heterogeneity. The same is responsible for the slight but evident decrease in the average values of the apparent strength. A noticeable scatter of the apparent tensile strength is caused (i) by the heterogeneity in distribution characteristics of the cell sizes in the given sample and, (ii) by fatal macroscopic material defects typical for this kind of material fabrication applied (fully filled cells, material absence over several cells etc.). The observed relations between the ceramic foam microstructure and measured apparent tensile strength confirm very good susceptibility of the measurements to microstructural differences however.

Table 1: Mean values and standard deviation of apparent tensile strength of ceramic foam specimens

specimen dimensions	label	σ_{fr} [MPa]	s (σ) [MPa]
10x10 mm^2	A	0.448	0.09
15x15 mm^2	B	0.321	0.04
30x30 mm^2	C	0.201	0.01
30x15 mm^2	T	0.313	0.06
30x15 mm^2 (sharp notch)	T-CR	0.130	0.03

The specimen size in the range of dimensions applied in this investigation affect the average values of tensile strength. The phenomenon is associated with statistical size effects, the higher loaded volume the lower strength value is measured. Note that all data sets tested here are possessing well the Weibull distribution as analysed elsewhere, Rehorek et al (2009). Nevertheless, some values were lying out of typical scatter. This is because of the above mentioned fatal defects in the microstructure. Either presence of filled cells representing more a bulk material behaviour than porous one on one side or absence of the material having the dimensions of several cells on the other side can lead to these differences.

3.2. Specimens with artificial central sharp notch

From macroscopic point of view the specimens with central artificial sharp notch simulating the crack showed similar behaviour as standard tensile test specimens. Fig. 2 shows characteristic load elongation trace. Each trace is typical by departure from the linearity (labelled by arrow 2) and unstable fracture after reaching the maximum load.

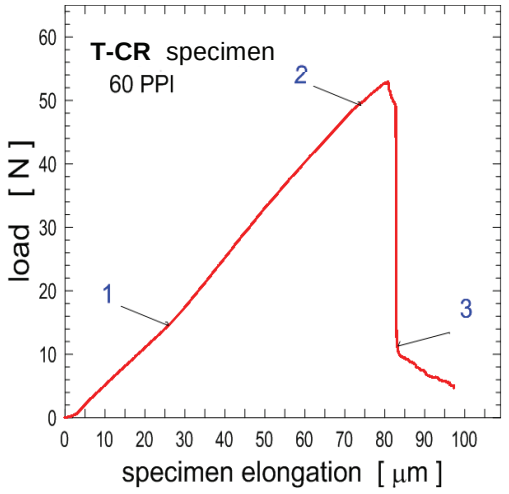

Fig. 2: Tensile load curves of T-CR specimen 15x30x60 mm^3 with internal through thickness crack of length 10 mm.

Note that the quasiplastic behaviour after stage 2 is not necessarily associated with the fracture of struts in the structure of the specimens. It could be attributed also to elastic opening of the artificial central sharp notch. Except for no direct evidence to the struts fracture at this stage there were no local displacements on the specimen surface

identified by digital image correlation technique that could correspond to the strut fracture inside the structure.

Fig. 3 shows views on specimen surface at three stages of loading identified in Fig. 2. The very first picture (left) shows the beginning of the elastic loading (note that the change in the slope of the linear elastic dependence is caused by the loading fixtures settlement). The central crack is seen very hardly because its thickness is less than one cell diameter. This configuration can be seen (and it is reflected also by data from digital image correlation) up to the point when the trace is departing from the linearity (point labelled by 2). After this stage the fracture process starts to develop very rapidly and results into configuration shown in Fig. 3 by the picture on the right side.

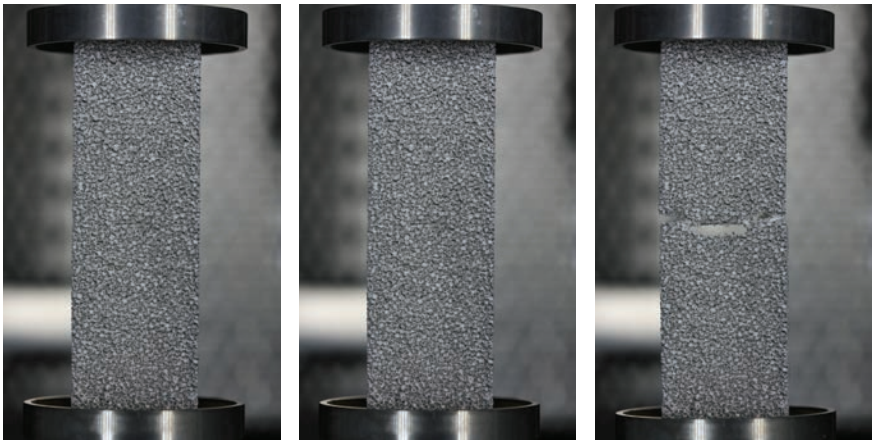

Fig. 3: Pictures of the T-CR specimen in loading stages show by arrows in Fig 2.

For the apparent strength calculation the maximum load was divided by the remaining unbroken area determined by image analysis from the fracture surfaces. It has been expected that the artificial central sharp notch cannot bear any load and the load is transferred by the un-cracked cross-section of the samples, i.e. by area having nominally dimension (2x) 10x15 mm^2. The obtained values including the average one and the scatter bands are shown in Fig. 4 and compared with the apparent strength values obtained from all other specimen geometries.

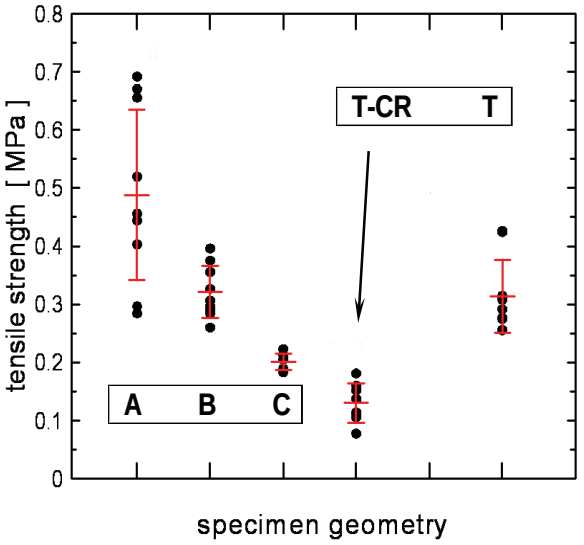

Fig. 4: Comparison of the average apparent strength values of specimens with different size and specimens containing central artificial sharp notch (T-CR).

It is evident that the fracture stress for the samples with central sharp notch is lowest of all the other specimen configurations, even in cases when the standard uncracked samples are possessing comparably higher cross-sectional area (loaded volume). The fracture surfaces were investigated for possible defects (filled cells, empty cells etc.) and/or for defects that could rise from the sharp notch preparation. There has been no such case observed and thus the very low fracture stress could be connected with additive local stress due concentration acting at the tip of the artificial sharp notch. Supposing this is a valid explanation an attempt has been made to calculate apparent crack tip stress intensity factor for the fracture conditions. Equation corresponding to the loaded flat panel with central crack was applied. For 10 samples tested the average value was $K_{IC} = 0.59 \pm 0.14$. The bulk material the specimens of which were fabricated from the same batch as the foam structures showed the values in the range of $K_{IC} = 2.12 \pm 0.44$. Chevron notch technique has been used to determine the fracture toughness in this particular case. From that point of view it seems that one could expect the stress concentration acting in the structure independently quite large unfilled space in the structure. The stress concentration phenomenon can be supposed up to certain cell size probably also in relation to the specimen size or number of cells in the uncrack area in front of artificial crack tip.

4. Conclusions

Specimens of different dimensions made of commercially available alumina foam ceramics Vukopor®A were tested in tension. The scatter of obtained data was observed being affected by occasional structure of ceramic foam and by inhomogeneities produced during manufacturing. The scatter is dependent on the specimen size and porosity type of the foam. With increasing sample size the scatter of measured data decreases. Dependence of apparent tensile strength on sample size of examined material was observed in the range of the investigated specimen dimensions.

Specimens containing hole-like defects inside have lower apparent tensile strength in comparison with defect free specimens. Also specimens having a central sharp notch simulating the crack showed comparable lower fracture loads and strength values than the samples without the sharp defect with the same loaded cross-sectional area. This leads to conclusion that there is real stress concentration effect of the internal crack which increases the local stress at the crack tip in causes fracture at nominal load lower than is needed for the regular foam structure fracture.

Acknowledgements

The works have been carried out in CEITEC centre - infrastructure supported by the project CZ.1.05/1.1.002/02.0068 financed from European Regional Development Fund. Support of Czech Science Foundation project Nr. GACR 14-11234S is further acknowledged.

References

Bertolla, L., Dlouhy, I., Philippart, A., Boccaccini, A. R., 2014a. Mechanical Reinforcement of Bioglass (R)-Based Scaffolds by Novel Polyvinyl-Alcohol/Microfibrillated Cellulose Composite Coating, Materials Letters 118, 204.

Bertolla, L., Dlouhy, I., Boccaccini, A. R., 2014b. Preparation and Characterization of Bioglass (R)-Based Scaffolds Reinforced by Poly-vinyl alcohol/Microfibrillated Cellulose Composite Coating. Journal of the European Ceramic Society 34, SI 3379.

Brezny, R., Green, D.J., 1990. The Effect of Cell Size on the Mech. Behaviour of Cellular Materials. Acta Metallurgica et Materialia, 38, 2517.

Brezny, R., Green, D.J., 1989. Fracture Behaviour of Open Cell Ceramics, Journal of the American Ceramic Society, 72, 1145.

Rezwan, K, Chen, Q.Z., Blaker, J.J. Boccaccini, A.R., 2006. Biodegradable and Bioactive Porous Polymer/Inorganic Composite Scaffolds for Bone Tissue Engineering, Biomaterials, 27, 3413.

Dawson, E.A. Barnes, P.A., Chinn, M.J., 2006. Preparation and Characterisation of Carbon-Coated Ceramic Foams for Organic Vapour Adsorption. Carbon 44, 1189.

Marcian, P., Majer, Z., Dlouhy, I., Florian Z., 2012. Estimation of Local Mech. Properties of Highly Porous Ceramics, Chemicke listy, 106, S476

Garrido, G.I., Patcas, F. C., Upper, G., Tuerk, M., Yilmaz, S., Kraushaar-Czarnezki, B., 2008. Supercritical Deposition of Pt on SnO(2)-Coated Al(2)O(3) Foams: Phase Behaviour and Catalytic Performance. Applied Catalysis A - General 338, 58.

Gibson, L.J., Ashby, M.F., 1999. Cellular Solids, Cambridge University Press, Cambridge.

Patcas, FC, Garrido, GI., Kraushaar-Czarnetzki, B., 2007. CO Oxidation over Structured Carriers: A Comparison of Ceramic Foams, Honeycombs and Beads. Chemical Engineering Science 62, 3984.

Rehorek, L., Dlouhy, I., Chlup, Z., 2009. Tensile Behaviour of Open Cell Ceramic Foams, Ceramics – Silikaty 53, 237.

Taslicukur, Z., Balaban, C., Kuskonmaz, N., 2005. Production of Ceramic Foam Filters for Molten Metal Filtration using Expanded Polystyrene. Journal of the European Ceramics Society, 27, 637.